Contents list available at IJRED website
Int. Journal of Renewable Energy Development (IJRED)
Journal homepage: http://ejournal.undip.ac.id/index.php/ijred

Research Article

Investigation of Electrochemical, Thermal and Electrical Performance of 3D Lithium-Ion Battery Module in a High - Temperature Environment

Snigdha Sharma[1,2], Amrish Kumar Panwar[2], Madan Mohan Tripathi[1*]

[1]Department of Electrical Engineering Delhi Technological University, Delhi-110042, India

[2]Department of Applied Physics, Delhi Technological University, Delhi-110042, India

ABSTRACT. In the present time, the rechargeable lithium-ion battery is being commercialized to meet the sustained market's demands. To design a more reliable, safe, and efficient Li-ion battery, a 3-D simulation study has been presented in this paper. In this study, a lithium-ion coin-cell is proposed which has $LiFePO_4$ as a positive electrode with a thickness of 1.76 µm, carbon as a negative electrode with a thickness of 2.50 µm and Celgard 2400 polypropylene sheet as a separator between the electrodes with a thickness of 2 µm. The proposed Li-ion battery has been designed, analyzed, and optimized with the help of Multiphysics software. The simulation study has been performed to analyze the electrochemical properties such as cyclic voltammetry (CV) and impedance spectroscopy (EIS). Moreover, the electrical and thermal properties at the microscopic level are investigated and optimized in terms of surface potential distribution, the concentration of electrolyte, open circuit, and surface temperature with respect to time. It has been noticed that the peak voltage, 3.45 V is observed as the temperature distribution on the surface varies from 0 ^{0}C to 80 ^{0}C at a microscopic scale with different C-rates. The analysis of simulation results indicates a smoother electrode surface with uniform electrical and thermal properties distribution resulting in improved reliability of the battery. The performed simulation and optimization are helpful to achieve control over battery performance and safe usage without any degradation of the environment. ©2020. CBIORE-IJRED. All rights reserved

Keywords: Lithium-ion battery, Electrolyte, Electrode, Current, Potential, Thermal model, Renewable Energy.

Article History: Received : July 23rd 2019; Revised: April 24th 2020; Accepted: April 30th 2020; Available online: May 1st 2020
Title of Manuscript: Sharma, S., Panwar, A.K. and Tripathi, M.M. (2020). Investigation of Electrochemical, Thermal and Electrical Performance of 3D Lithium-Ion Battery Module in a High -Temperature Environment. *Int. Journal of Renewable Energy Development*, 9(2),151-157
https://doi.org/10.14710/ijred.9.2.151-157

1. Introduction

Recently, Non-renewable sources of energy such as coal, crude oil, (Dominic et al. 2010) and many more are depleting and leading to hazardous problems in the environment such as greenhouse gas emission, global warming, (Li et al. 2013) and emission of pollutants like carbon dioxide (CO_2), Nitrogen oxides (NO_2), sulfur dioxide (SO_2) and various particulate matters (PMs) (Majeau-Bettez et al. 2011). In the context of these problems, researchers look towards the replacement of energy sources which helps in enhancing the environment condition and cause less health-hazardous to nature (Thomas et al. 2011). Hence, to cater to the growing demand for energy and making the environment compatible, it is essential to explore energy storage and conversion devices resources. In the recent past, the rechargeable batteries are in focus for energy storage and conversion devices worldwide and among rechargeable batteries: Lithium-ion batteries are being commercialized to due high energy and power densities (Kang et al. 2013). These batteries are not only preferable for portable electronics but also prove its potential towards the large-scale electricity storage on smart grids, the automotive industry in terms of electric vehicles (EVs) (Zaghib et al. 2005), aerospace engineering, communication, back-up and many more (Thierry et al.1998).

Battery consumption is increasing worldwide on a large scale for various purposes and dependency on battery has been continuously increasing (Thierry et al.1998). Traditionally Li-ion batteries are thought to be very complicated which undergoes various electrochemical and mechanical changes during its working condition. This paper presents the design, simulation, and analysis of a Li-ion battery which takes care of these issues. To overcome the issues of Li-ion battery and for making these batteries more reliable and safer, a 2D and 3D simulation has been performed using a computer model in Multi-physics software to explore the battery behavior and optimize the characteristics of the battery (Long et al. 2011). The experimental data is used to construct a theoretical model to investigate the electrochemical, electrical, and thermal properties of the lithium-ion battery (Andreas Nyman et al. 2012). The Multi-physics software helps to develop the physics-based model and

* Corresponding author: mmmtripathi@gmail.com

then determines the working mechanism of the lithium-ion battery for improving different properties in the battery (Farid et al. 2017). In addition, the simulation also helps to investigate the temperature variance with respect to time, electrolyte potential, ion concentration on the surface, and electrolyte salt concentration (Samu et al. 2015). Therefore, in this work, a computational technique has been used to diagnose the battery characteristics directly through software without any environmental degradation.

The remaining paper is organized as follows. Section 2 describes the geometry and formulation of lithium-ion battery and it also describes the model parameters. In section 3, the model optimization results are presented and also analyze the battery characteristics of the different environmental conditions. Further, the conclusion is summarized in section 4.

2. Model Geometry and Formulation

2.1 Lithium-ion battery model formulation

In this work, a Lithium Iron Phosphate ($LiFePO_4$) battery is used for computational analysis. A 3-D structure model is designed with the help of three basic parameters such as electrochemistry kinetics, transport phenomena, and thermodynamics. The proposed 3-D structure of a battery is divided as a positive electrode, a negative electrode, electrolyte, separator, and the current collector (CC). This structure has been demonstrated in the Fig.1. Here, the outermost layer of both the sides in the battery is represented as a positive (Aluminium) and negative (Copper) current collector and the inner layer in contact (coated) with current collectors is represented as a positive ($LiFePO_4$) and the negative (carbon) electrodes, respectively.

Moreover, a separator made of a microporous polypropylene sheet (Celgard 2400) is kept between both of these electrodes. Further, the liquid electrolyte, $LiPF_6$ is filled inside the battery that promotes the movement of ions from positive electrode (LFP) to negative electrode (Carbon) during the charging and reverses process during discharging. This construction helps to solve the electrolyte concentration within the porous electrodes and electrolyte potential within the separator.

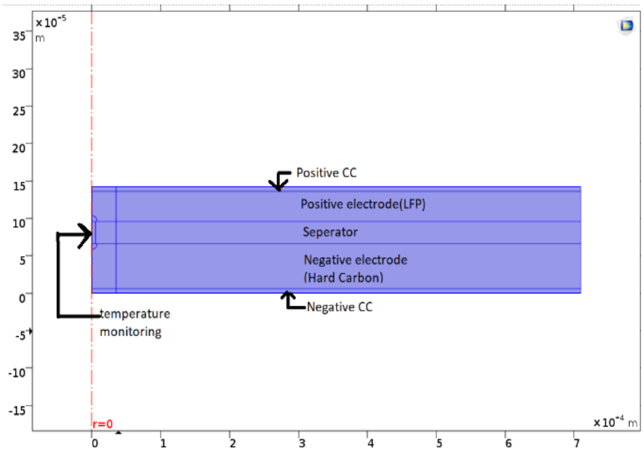

Fig. 1 Geometry of Lithium-ion Battery model

In this lithium-ion battery formulation, different types of characterization techniques have been performed on Li-ion batteries. First, the electrochemical characterization techniques (Mingzhi et al. 2018) have been performed with the help of the electroanalysis method (Parmender et al. 2014). Electrochemical techniques are further elaborated in two methods i.e. cyclic voltammetry (CV) and Electrochemical impedance spectroscopy (EIS). In this process, the model used contains a 2-D axisymmetric domain surrounded by infinite elements, that comprises of the pseudo-two-dimensional electrochemical structure (Kotub et al. 2016). Table 1 represents the domain equation and boundary conditions for this formulated model.

Table 1.
Summary of domain equation and boundary conditions.

Method	Domain Equations	Boundary Condition
Cyclic Voltammetry	$\nabla.(Di\ \nabla ci) = 0$	$\eta = \phi_s - Eeq$
Electrochemical Impedance Spectroscopy	$\frac{\partial C_i}{\partial t} = \nabla.(Di\ \nabla ci)$ (Fick's second law)	$-n \cdot N_i = \frac{v_i i_0 c}{nF}$ Faraday's law of electrolysis

Table 2.
Electrical and thermal properties for battery

Parameter	$LiFePO_4$	Carbon	$LiPF_6$	Al CC	Cu CC
Diffusion Coefficient (m^2s^{-1})	$1.8 \cdot 10^{-14}$	$3.4 \cdot 10^{-14}$	$1.4 \cdot 10^{-13}$	-	-
Electrical Conductivity(S/m)	$3.7 \cdot 10^{-9}$	$2.5 \cdot 10^{-6}$	$1 \cdot 10^{-7}$	$3.7 \cdot 10^{7}$	$5.96 \cdot 10^{7}$
Thermal Conductivity(W(m.k))	3.4	1	0.15	400	238
Young Modulus (Pa)	$4.9 \cdot 10^{9}$	$4.1 \cdot 10^{9}$	-	$110 \cdot 10^{9}$	$70 \cdot 10^{9}$
Density (Kg/m^3)	3600	2260	940	8960	2700
Heat Capacity(J/Kg.k)	2500	881	1046	385	900

The other characterization techniques used were electrical and thermal characterizations where various other parameters were used for the formulation of the battery model. Some important parameters for electrical and thermal characterizations were demonstrated in Table 2. These parameters help to obtain the electrical and thermal characteristics of the lithium-ion battery model.

2.2 Lithium-ion battery model parameters

In this section, the design of the lithium-ion battery is presented on the coin-cell model. The model parameters from the coin-cell of lithium-ion have been formulated with the help of simulation. Certain parameters have been taken as a 'standard value from literature (Mingzhi et al. 2018), whereas certain parameters such as cell dimension, electrode thickness, and many more have been referenced from a fabricated 2032-coin cell by Mingzhi et al. (2018). Moreover, the stoichiometry of both positive and negative mass transfer coefficient and the electrolyte charge transfer coefficient have been taken as a known parameter from the literature (Hellwig et al.2011). Selective parameters of fabricated 2032-coin cell models are explained in Table 3.

Table 3.
Measured and Identified Parameters for the Lithium-Ion Battery Model Simulation

Parameter	Units	Value	Description
E_cell	V	3.4	Cell Potential
L_tot	m	$1.42*10^{-4}$	Cell total Thickness
epsl_sep	-	0.4	Porosity of separator
$T_{initial}$	K	328	Initial Temperature
T_{final}	K	395	Final Temperature
Maximum electrodeSOC	SOCmax	0.79	Operational SOC
Minimum electrode SOC	SOCmin	0.02	Operational SOC
I_disch	i_1C(A/m^2)	17.5	Discharge current
T_disch	Seconds	2000	Discharge duration
I_charge	-i_1C(A/m^2)	-17.5	Charge current
T_charge	Seconds	2000	Charge duration
C	-	1	C-rate factor

The above parameters are taken as operational parameters for simulation analysis. These were the maximum number of parameters that identified theoretically in the lithium-ion battery model predicted by (Smith, 2006).

2.3 Mesh and Optimization Analysis

In this section, the simulation study helps to demonstrate the time-dependent 3D Li-ion battery model, which was formulated and designed on a COMSOL Multiphysics 5.3 version. The input and operational parameters were already explained above for forming the physics of the battery. In this, 3D simulation various electrochemical characteristics were analyzed using the mathematical Butler-Volmer equation and also calculated the Li-ion diffusion from Faraday's Law. Initially, the lithium-ion domain was specified using the electrode for electronically conducting medium, in which different material was specified according to the various parameters. Then, all domains were specified at its specific material parameters and also set with heat transfer part in all domains. The step function to ramp function was set up for providing electric conductivity in the penetrating filament. At last, meshing was created with the help of triangular mesh, which was fitted close to the penetrating filament, and the mapped mesh was used in the remaining domain with a growing element size in the x-direction. In Figure 2, the meshing structure represents a blue dotted line and black dotted line, in which blue dots show the mapped mesh for all domains, and black dots show the triangular mesh only in penetrating filament.

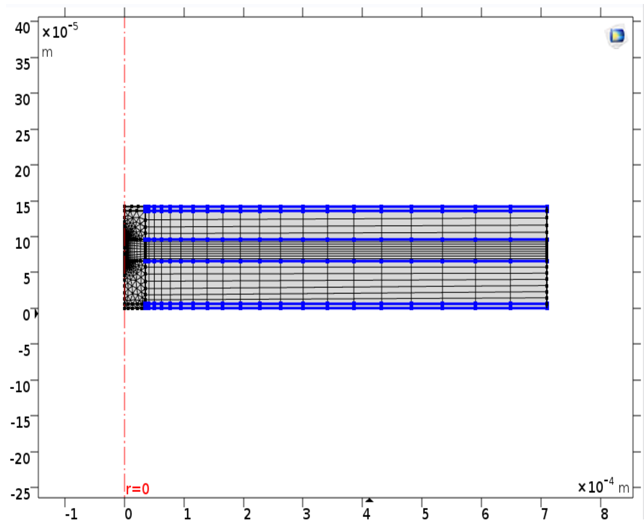

Fig. 2 Meshing Structure of 3D Lithium-ion Solid State Model

After setting the physics geometry and meshing in the Li-ion battery model. Further, the model was to be solved in two steps. In the First step, the battery cell was initialized, in which heat transfer in solid-state was turned off in the first solver step. In the second step, the parametric sweep was used on the radii of the penetrating filament. Hence, after that simulation results were plotted with the help 3D and 1D plot groups as shown in the next section.

3. Results and Discussion

In this section, the simulation results have been investigated. During the simulation of the coin-cell type Li-ion battery, the characteristics of the battery under the influence of different operating conditions have been observed and explained. All the results are analyzed at different boundary conditions and illustrated with a brief description.

3.1 Electrochemical Characterization

A) Cyclic Voltammogram (CV)

The CV was performed under the influence of quasi-static approximation with the help of an electroanalytic technique (Tao et al. 2007). In this method, a microdisk electrode was designed in which surface concentration present on the surface of the electrode that was almost equally distributed. Figure 3 demonstrates the surface concentration for mass transport controlled oxidation species. This result helps to investigate the uniform distribution of potential over the surface of the electrode and also and also signifies that the concentration gradients become linear and tend to move the Li-ions more freely through the electrolyte due to the high diffusion rate.

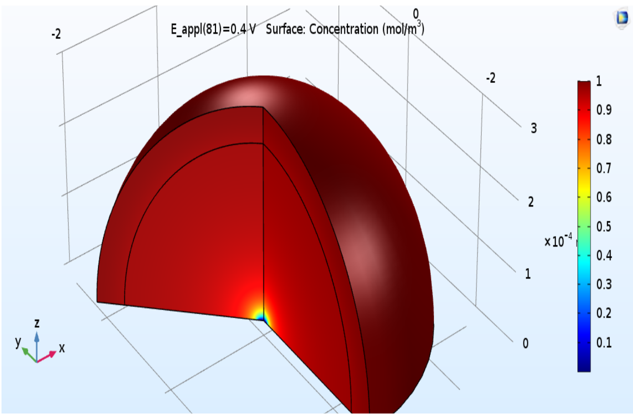

Fig. 3 Surface concentration at a microdisk electrode (3-D cross-section model)

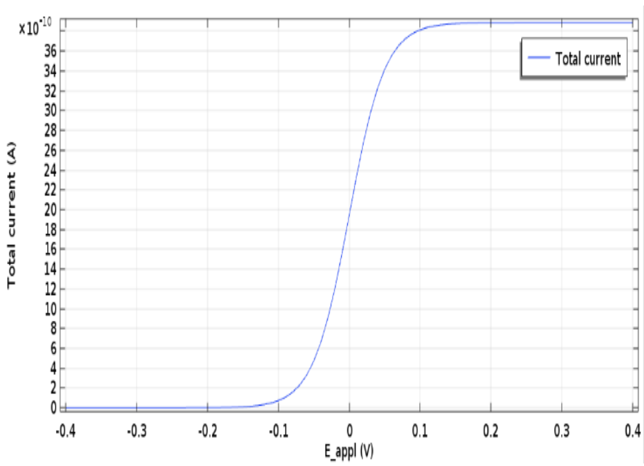

Fig. 4 Steady-State Cyclic Voltammogram at a Microdisk Electrode

Further, Figure 4 represents the variation of current and voltage under steady-state conditions. Initially, the current was negligible because the oxidation reaction does not take place due to the reducing potential. As the potential increases, the oxidation reaction takes place during the charging process. The ionic transport mechanism is generally associated with macroscopic diffusion or related to the movement of Li ions when the external electric potential was applied on the battery. Similarly, the current also starts increasing during this phenomenon (Tommy et al. 2012). Once the oxidation takes place, the current becomes stable and limits the rate of Li-ion transport species towards the working electrode and then it demonstrates the relation between electrode kinetics and chemical species of Li-ion.

B) Electrochemical Impedance Spectroscopy (EIS)

EIS is used to study the harmonic response of a battery. In this method, real and imaginary impedance value reveals the kinetic and mass transport properties of the coin-cell battery and also explains the capacitive properties of the Li-ion battery (Smith et al. 2006).

Figure 5 shows the relationship between real and imaginary impedance with a variable frequency range. This result has been analyzed at a very-low-frequency range of ko=0.001 cm/s in which mass transport always dominates through which semi-circle obtained. Whereas, at a high-frequency range of ko=0.1cm/s, the transition to kinetic control occurs at which straight line obtained on the curve.

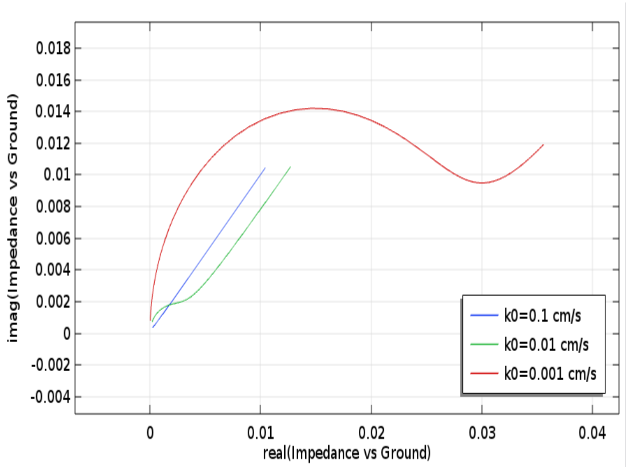

Fig. 5 Nyquist plot at a various range of frequency

The above Nyquist plot represents to extract the ohmic resistance in the electrolyte during the measurements. The red color semi-circle in the plot represents the kinetic resistance of the electrode and the Tafel slope was obtained, when the diameter was divided by the current density and it shows the uniform current distribution across the thickness of the electrode.

At high frequency, the plot implies a very low impedance, which means that the alternating current is transferred between the electrode and the electrolyte at a very close position of the interface. Similarly, in figure 6 represents the bode plot at various frequency ranges in which magnitude and phase angle was plotted through which reaction proceeds under the kinetic and mass transport control species at a heterogeneous constant.

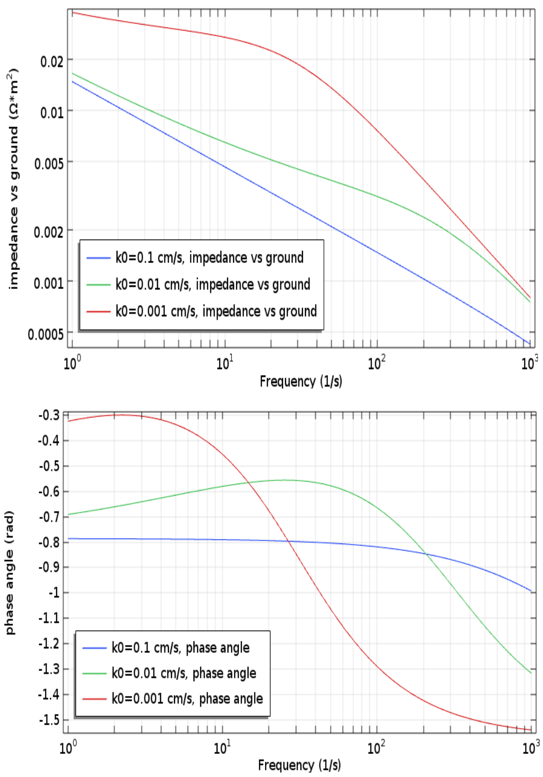

Fig. 6 Bode plot: (a) Magnitude of impedance, (b) Phase angle of the complex impedance at a various frequency range

3.2 Thermal Characterization

In this, a 3-D coin-cell type model was developed in which a penetrating filament (named as temperature monitoring) used to raise the temperature of the cell which was connected through the separator between the two electrodes (Yonghuang et al. 2012). The initial temperature of the cell is 295 K and it attains a maximum temperature of 335 K during the charging-discharging process as observed by simulation.

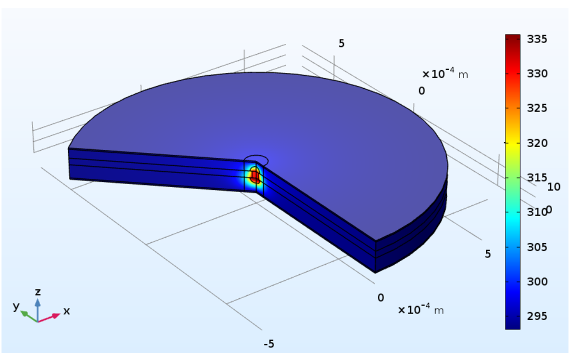

Fig. 7 Temperature distribution over the surface after 0.1 s

Figure 7 represents the temperature distribution over the surface after the 0.1 s of the simulation time. Initially, the temperature filament conductivity is set very low after it ramped towards the full conductivity. This 3D revolution plot shows that the maximum temperature was located close to the penetrating filament and the temperature change was confined to a small space close to the filament and rest on the surface the temperature is equally distributed which shows a good thermal property of a coin-cell battery.

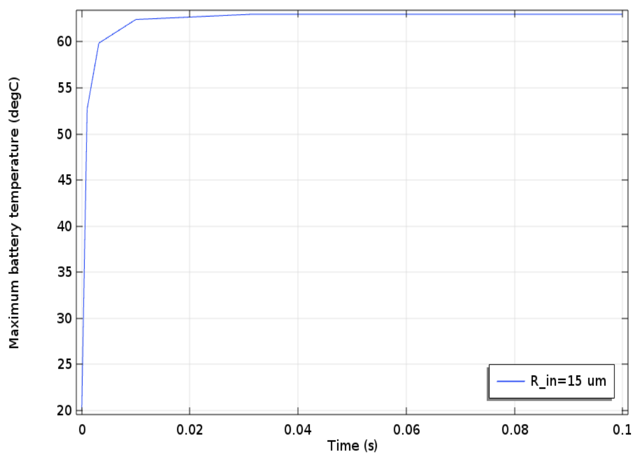

Fig. 8 Temperature variation with respect to time

Figure 8 represents the 1D plot of temperature vs time, in this curve, the maximum temperature across the radius of the cell was above 60 degrees Celsius and as the temperature reaches its maximum range after a certain time it becomes constant and uniform over the surface of the electrode. Hence, it represents that the battery material has good thermal stability in a high-temperature environment.

3.3 Electrical Characterization

In this investigation, the model used certain boundary conditions, and to keep the electronic current balance inside the battery, negative current collector potential has been kept 0 V, whereas, at the positive current collector, the current density is set. In this, the current density is cycled through the discharge cycle in which the current is set at zero interval initially and then move towards the final charging stage (Thanagasundram et al. 2012).

Figure 9 demonstrates the ionic conductivity of the electrolyte using an interpolation function, in which conductivity directly depends upon the equilibrium potential of the positive and negative electrode. This function varies according to the charge and discharge phenomena because of the change in the material composition.

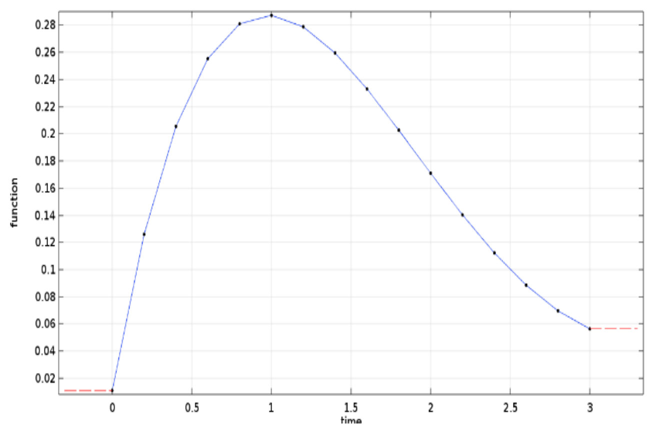

Fig. 9 Ionic conductivity of the electrolyte using an interpolation function

As the interpolation function depends upon the concentration of the electrolyte. Hence, as the surface concentration varies the equilibrium voltage also varies and tends to cause a lower reaction overpotential. It also leads to a decrease in the current density, which affects voltage loss in the battery.

Furthermore, Figure 10 demonstrates the electrolyte salt concentration at various times such as 600 s, 1200 s, 1800 s, and 2200 s. This curve is plotted during the operation of the cell in which the cell experiences a sudden steep in voltage due to the low effective diffusion coefficient in the electrolyte. This, in turn, leads to variation in electrolyte concentration and ionic conductivity.

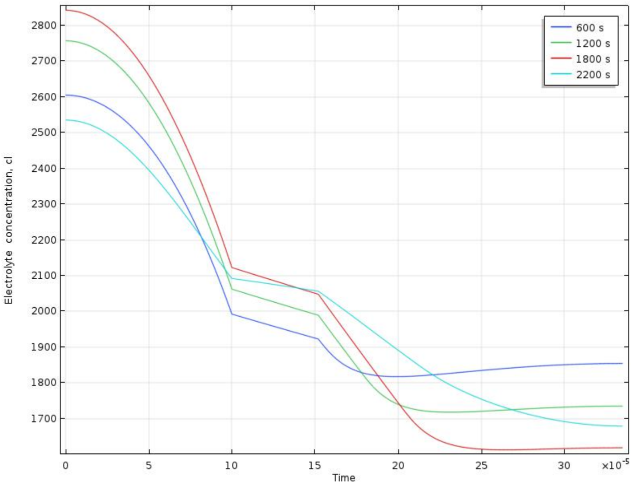

Fig. 10 Electrolyte salt concentration at various times

The salt concentration of the electrolyte in the solid phase at the surface of the electrode also affects the current density of the electrode, which in turn results from the poor electrolyte conductivity.

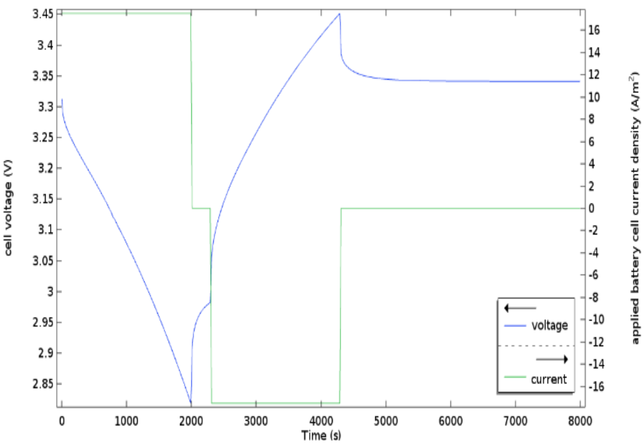

Fig. 11 Cell current and voltage during the charge and discharge cycle

Figure 11 represents the voltage and current curve during the charge-discharge cycle. This plot is obtained at a nominal current of a 1C rate. Initially, the cell is discharged at 1C rate for the 2000 s then the circuit remains open for 300 s. After that, the cell is again charged for the 2000 s than it is completely left as an open-circuit. It has been noticed from the result that there are losses visible in the curve due to the immediate relaxation of the voltage. Firstly, there has been observed an ohmic loss in the voltage curve of 100 mV approximately due to the holding of the charge for 300 s. When the current value is kept zero. Secondly, the concentration overpotential has also been observed at a relaxation time of about 50 mV.

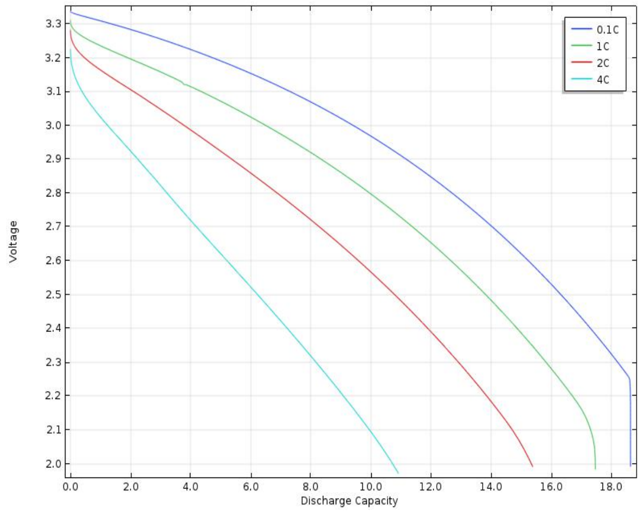

Fig. 12 Discharge curve at various C-rate

Variation of discharge capacity at different C rates such as 0.1C, 1C, 2C, and 4C are shown in Fig. 12. In this curve, when the cell voltage drops below 3 V then the maximum discharge capacity has been analyzed at 1C rate and hence the discharge capacity decreases dramatically. Further, when we analyzed at a 4C rate then the battery discharge capacity is 50% of the theoretical capacity before 3V.

4. Conclusion

In this study, 3-D models of coin-cell type lithium-ion batteries are simulated using multi-physics software. It has been observed that the electrochemical characterization, cyclic voltammetry curve indicates current becomes constant after a certain voltage, 0.2 V. Hence, it reveals the controlled transport behavior of species. Moreover, the EIS analysis shows the real component corresponds to resistance in-phase, and the imaginary component corresponds to reactance 90^{o} out-of-phase for the applied voltage as well as good electrochemical behavior at the high and low-frequency range. In the thermal analysis, surface resistant behavior at high temperature was equally distributed and shows better thermal stability. In the electrical characterization, it has been noticed that variation in electrolyte concentration reveals the low diffusion coefficient and low ionic conductivity in the cell at a nominal C-rate. The charging-discharging process showing ohmic and concertation losses in the battery.

Acknowledgment

Authors are thankful to DTU for providing financial assistance through the "DTU research project grant: DTU/IRD/619/2019/2114" in LIBT Lab, Department of Applied Physics, Delhi Technological University, New Delhi for providing support to carry out this research work.

References

Bahiraei, F., Ghalkhani, M., Fartaj, A., and Nazri, G., (2017) A pseudo-3D electrochemical-thermal modeling and analysis of a lithium-ion battery for electric vehicle thermal management applications," Applied Thermal Engineering 125, 904-918.

Cai, L., and White, R., (2011) Mathematical modeling of a lithium-ion battery with thermal effects in COMSOL Inc. Multiphysics (MP) software, Journal of Power Sources 196 (14), 5985-5989.

Cassagneau, T., and Fendler, J., (1998) High-density rechargeable lithium-ion batteries self-assembled from graphite oxide nanoplatelets and polyelectrolytes, Advanced Materials 10 (11), 877-881.

Dai, M., Huo, C., Zhang, Q., Khan, K., Zhang, X., and Shen, C., (2018) Electrochemical Mechanism and Structure Simulation of 2D Lithium-Ion Battery," Advanced Theory and Simulations 1 (10), 1800023.

Kang, D. H.P., Chen, M., and Ogunseitan, Oladele., (2013) Potential environmental and human health impacts of rechargeable lithium batteries in electronic waste, Environmental science & technology 47 (10), 5495-5503.

Hellwig, C., Sorgel, S., and Bessler, W., (2011) A multi-scale electrochemical and thermal model of a LiFePO4 battery, ECS Transactions 35 (32), 215-228.

Jiang, T., Zhang, S., Qiu, X., Zhu, W., and Chen, L., (2007) Preparation and characterization of silicon-based three-dimensional cellular anode for lithium-ion battery, Electrochemistry communications 9 (5), 930-934.

Kukkonen, S., Erkkila, V., Manninen, A., Haavisto, J., and Pihlatie, M., (2015) Method for dimensioning battery and thermal management systems for heavy-duty vehicle applications using aged battery experimental data and advanced modeling techniques, ECS Transactions 68 (2), 83-95.

Li, L., Dunn, J., Zhang, X., Gaines, L., Chen, R., Wu, F., and Amine, F., (2013) Recovery of metals from spent lithium-ion batteries with organic acids as leaching reagents and environmental assessment, Journal of Power Sources 233, 180-189.

Majeau-Bettez, G., Hawkins, T., and Stromman, A (2011) Life cycle environmental assessment of lithium-ion and nickel-metal hydride batteries for plug-in hybrid and battery electric vehicles, Environmental science & technology 45 (10), 4548-4554.

Notter, D., Gauch, M., Widmer, R., Wager, P., Stamp, A, Zah, R., and Althaus, H., (2010) Contribution of Li-ion batteries to the environmental impact of electric vehicles.

Nyman, A., Ekstrom, H., and Fontes, E., (2012) Modeling the Lithium-ion battery," IEEE Spectrum: Technology & Science.

Smith, K., (2006) Electrochemical modeling, estimation, and control of lithium-ion batteries.

Smith, K., and Wang, C., (2006) Power and thermal characterization of a lithium-ion battery pack for hybrid-electric vehicles, Journal of power sources 160 (1), 662-673.

Singh, P., Khare, N., and Chaturvedi. P, "COMSOL Modelling for Li-ion Battery Diagnostics, 2014.

Thanagasundram, S., Arunachala, R., Makinejad, K., Teutsch, T., and Jossen, A., 2012 (unpublished) presented at the European Electric Vehicle Congress.

Uddin, K., Perera, S., Widanage, W., Somerville, L., and Marco, J., (2016) Characterising lithium-ion battery degradation through the identification and tracking of electrochemical battery model parameters, Batteries 2 (2), 13.

Wanger, T., (2011) The Lithium future—resources, recycling, and the environment, Conservation Letters 4 (3), 202-206.

Ye, Y., Shi, Y., Cai, N., Lee, J., and He, X., (2012) Electro-thermal modeling and experimental validation for lithium-ion battery, Journal of Power Sources 199, 227-238.

Zaghib, K., Charest, P., Guerfi, A., Shim, J., Perrier, M., and Striebel, K., (2005) LiFePO4 safe Li-ion polymer batteries for clean environment, Journal of power sources 146 (1-2), 380-385.

Zavalis, T., Behm, M., and Lindbergh, G., (2012) Investigation of short-circuit scenarios in a lithium-ion battery cell, Journal of The Electrochemical Society 159 (6), A848-A859.